PHYSICAL REVIEW A **78**, 031801(R) (2008)

Observation of diffraction-managed discrete solitons in curved waveguide arrays

Alexander Szameit,[1] Ivan L. Garanovich,[2] Matthias Heinrich,[1] Alexander Minovich,[2] Felix Dreisow,[1]
Andrey A. Sukhorukov,[2] Thomas Pertsch,[1] Dragomir N. Neshev,[2] Stefan Nolte,[1]
Wieslaw Krolikowski,[2] Andreas Tünnermann,[1] Arnan Mitchell,[3] and Yuri S. Kivshar[2]
[1]*Institute of Applied Physics, Friedrich-Schiller-University Jena, Max-Wien-Platz 1, 07743 Jena, Germany*
[2]*Nonlinear Physics Centre and Laser Physics Centre, Centre for Ultra-high Bandwidth Devices for Optical Systems (CUDOS), RSPhysSE, Australian National University, Canberra ACT 0200, Australia*
[3]*School of Electrical and Computer Engineering, RMIT University, Melbourne VIC 3001, Australia*
(Received 24 April 2008; published 15 September 2008)

We observe the formation of discrete diffraction-managed optical solitons in arrays of periodically curved coupled waveguides for two types of modulated structures: laser-written arrays in silica glass with self-focusing nonlinearity and lithium niobate waveguide arrays with self-defocusing photorefractive nonlinearity. Our results demonstrate that, for both types of nonlinear response, soliton formation occurs after transitional self-induced beam broadening, being fundamentally different from nonlinear self-focusing and defocusing in a bulk medium or discrete self-trapping in straight waveguides.

DOI: 10.1103/PhysRevA.78.031801 PACS number(s): 42.65.Jx, 42.65.Tg, 42.82.Et

Propagation of light in nonlinear dielectric media with a periodically varying refractive index exhibits many different features, which do not occur in homogeneous nonlinear materials [1]. The underlying periodicity can strongly modify the physics of nonlinear beam self-action, where both self-focusing and self-defocusing nonlinear responses can lead to beam self-trapping in the form of discrete spatial solitons [2,3]. On the other hand, it was shown that the beam spreading due to linear diffraction can be fully suppressed in curved or transversely modulated waveguide arrays due to the effect of optical Bloch oscillations [4–6], similar to the Bose-Einstein condensates (BECs) in optical lattices, where atomic Bloch oscillations can occur as a result of a constant force due to gravity or lattice acceleration [7]. More flexible control over the linear beam propagation is realized when the waveguide bending is modified periodically, allowing one to either completely cancel the diffraction or reduce it by an arbitrary fraction [8–12], in analogy to the dynamic localization of charged particles in ac electric fields [13].

The recent theoretical studies of nonlinear beam propagation in lattices with modified linear diffraction predicted that solitons can be generated in various types of diffraction-managed lattices, including periodically curved waveguide arrays [14,15] and other types of modulated one- and two-dimensional photonic structures [16,17], and it was found that they are reminiscent of dispersion-managed temporal solitons [18–20]. On the other hand, many properties of discrete diffraction-managed solitons may be completely different. In particular, numerical simulations indicate that narrow beams propagating in arrays of curved waveguides with reduced diffraction should exhibit nonlinear self-trapping to discrete solitons at increased powers [15,16], similar to the dynamics of a particle in a nonlinear chain under the action of a dc field [21]. At intermediate power levels, nonlinearity may instead lead to beam broadening due to the destruction of periodic linear beam refocusing. Whereas nonlinear destruction of Bloch oscillations and the associated beam broadening was demonstrated experimentally in optical waveguide arrays [5], and recently also in atomic BECs with Feshbach resonance management [7], the observation of the theoretically predicted beam refocusing and soliton formation at stronger nonlinearities remained an open problem.

In this work, we present the experimental observation of discrete diffraction-managed spatial optical solitons in arrays of periodically curved waveguides. To demonstrate generality of soliton generation, we perform experiments in two structures with distinctly different nonlinear response: (i) femtosecond laser-written waveguide arrays in silica glass with self-focusing nonlinearity, and (ii) arrays created by titanium indiffusion in lithium niobate ($LiNbO_3$) crystals with self-defocusing photorefractive nonlinearity. We demonstrate that, in both cases, the beam exhibits transitional broadening at intermediate powers, followed by a sharp transition to strong localization above a certain power threshold.

In our experiments, we create waveguide arrays with a sinusoidal axis bending profile of the form $x_0(z) = A[\cos(2\pi z/L) - 1]$, where $x_0(z)$ is the transverse lattice shift as a function of the propagation distance z, and A and L are the waveguide axis bending amplitude and period, respectively. When the bending amplitude A is such that $2\pi\omega A/L = \xi$, where ω is the normalized frequency and $\xi \simeq 2.40$ is the first root of the Bessel function J_0 [10,15], the effective beam diffraction is canceled after propagation over each bending period L, in close analogy to the dynamic localization of charged particles in ac electric fields [13]. The normalized frequency is $\omega = 2\pi n_0 d/\lambda$, where λ is the vacuum wavelength, n_0 is the average refractive index of the medium, and d is the spacing between the centers of the adjacent waveguides.

First, we study arrays of curved self-focusing waveguides fabricated in fused silica by femtosecond laser writing [22]. We use samples with four different waveguide spacings, $d = 34$, 36, 38, and 40 μm. The waveguide bending amplitudes are chosen to satisfy the dynamic localization condition, $A = 104$, 98, 93, and 88 μm, respectively. Each sample is $L = 105$ mm long and consists of 13 waveguides with elliptical transverse cross section of approximately 4×13 μm^2 [23]. At the input, 150 fs laser pulses at the wavelength $\lambda = 800$ nm are coupled to the central waveguide. The measured pulse width at the output is about 200 fs, indicating

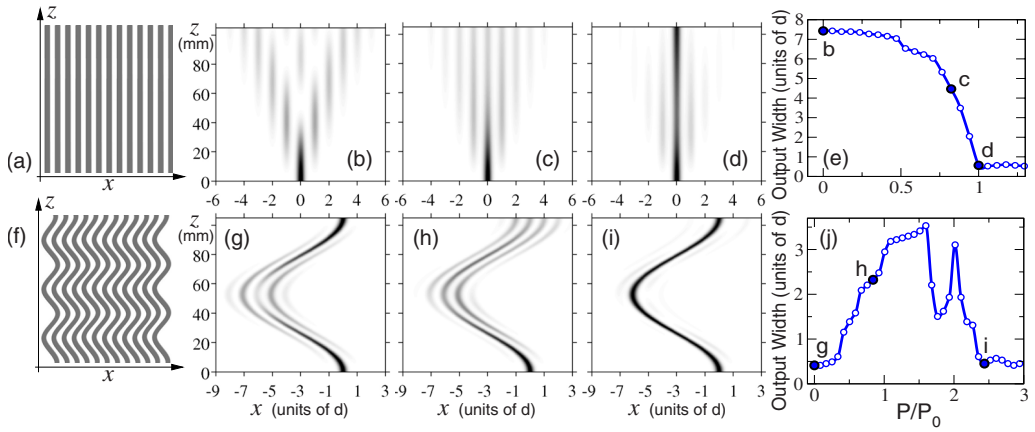

FIG. 1. (Color online) Numerical simulations of beam propagation in (a) straight and (f) periodically curved nonlinear waveguide arrays. (b), (c), (d) Discrete diffraction, beam self-focusing, and lattice soliton formation in a straight array. (g), (h), (i) Dynamic localization, transitional beam broadening, and diffraction-managed soliton formation in a curved array. (e), (j) Output beam width vs the input power for straight and curved arrays, respectively. Points *b*, *c*, *d*, and *g*, *h*, *i* correspond to the input powers in (b), (c), (d) and (g), (h), (i), respectively. Input power is normalized to the power threshold for the lattice soliton formation in the straight array. Parameters correspond to fabricated structures in silica glass with waveguide spacing 34 μm.

that pulse broadening due to dispersion has no significant impact on the pulse peak power [24].

In order to underline the key features of the discrete diffraction-managed solitons, we perform numerical simulations of beam self-action in periodically curved nonlinear waveguides using discrete equations for the mode amplitudes of individual waveguides [15]. In straight waveguides [see Fig. 1(a)], one observes monotonic beam self-focusing as the input power increases [see Figs. 1(b)–1(e)]. However, the beam dynamics becomes completely different in periodically curved waveguides [sketched in Fig. 1(f)] with canceled effective diffraction. Whereas at low input powers the input beam profile is restored after each modulation period [Fig. 1(g)], the beam broadens as the power is increased [Fig. 1(h)]. This effect is analogous to the nonlinear destruction of Bloch oscillations [5,7,16,21]. At higher powers, above a well-defined threshold, discrete self-trapping and formation of diffraction-managed lattice solitons occurs [Fig. 1(i)]. The dependencies of the output beam width on the input power in straight and curved waveguide arrays is shown in Figs. 1(e) and 1(j), respectively. Whereas in the case of straight waveguides the output width decreases *monotonically* with power, in curved waveguides we observe complex nonmonotonic power dependence of the output beam width.

We now test these theoretical predictions experimentally. In straight waveguide arrays, we observe monotonic beam self-focusing as we increase the input power, leading eventually to the formation of a single-site lattice soliton at some threshold power level [3] (see Fig. 2). In agreement with previous studies [1], the soliton power is lower for the samples with larger waveguide spacing, for which the coupling between the waveguides is weaker [see Figs. 2(c) and 3(a)].

Next, we study light propagation in curved waveguides for different input powers. At low powers (linear regime), we observe dynamic localization of light in the curved waveguides, as in [8,10,11]. Indeed, at the output facet of the arrays all the light is collected back into the same central waveguide in which it was coupled initially at the input [see Figs. 4(a) and 4(b), top].

When the input power is increased, we observe transitional beam broadening, in agreement with the numerical simulations above. The beam experiences significant self-induced broadening [see Figs. 4(a) and 4(b), $P \sim 1$ MW] because the nonlinearity destroys the dynamic localization condition by changing the refractive index of the waveguide material. With propagation, the beam broadens and its intensity is reduced accordingly, such that the effect of the nonlinearity becomes weaker. Since linear discrete diffraction is fully suppressed in our curved waveguide arrays, the beam broadening stops when the average beamwidth reaches a certain value.

Then, at higher input powers, nonlinear self-trapping of the beam to a single lattice site occurs, and we observe formation of discrete diffraction-managed spatial optical solitons [see Figs. 4(a) and 4(b), bottom]. Whereas a similar

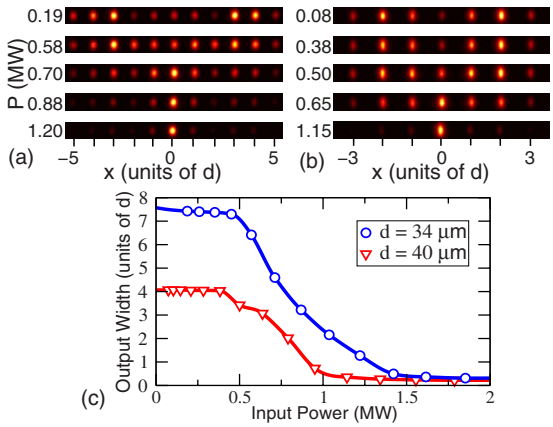

FIG. 2. (Color online) (a), (b) Output beam profiles as a function of input peak power, measured in straight laser-written waveguide arrays with waveguide spacing d=(a) 34 and (b) 40 μm. (c) Output beamwidth vs input power. Circles correspond to (a), triangles to (b).

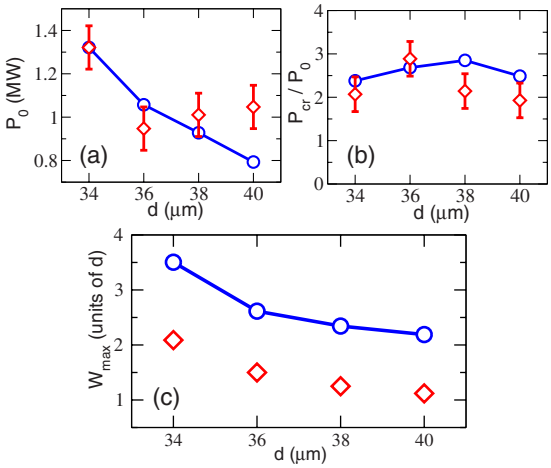

FIG. 3. (Color online) (a) Peak laser power P_0 required for the formation of a single-site lattice soliton in straight waveguide arrays, and (b) critical power P_{cr} required for the formation of diffraction-managed solitons in curved waveguide arrays, as a function of the waveguide spacing d. Diamonds and circles represent the measured and the calculated data, respectively. In (b) powers of the diffraction-managed solitons in curved arrays are normalized to powers of the lattice solitons in straight arrays of the same d. (c) Measured (diamonds) and calculated (circles) maximum nonlinear beam broadening for curved waveguide arrays with different waveguide spacing.

transition from nonlinear delocalization to self-trapping was predicted for Bloch oscillations [16], it was not observed in previous experiments [5,7]. We find, in good agreement with the theoretical predictions [15], that the power required for the formation of the diffraction-managed solitons in curved waveguide arrays is more than two times higher than the critical power of lattice solitons in exactly the same but straight waveguide arrays [compare Fig. 4(c) with Fig. 2(c);

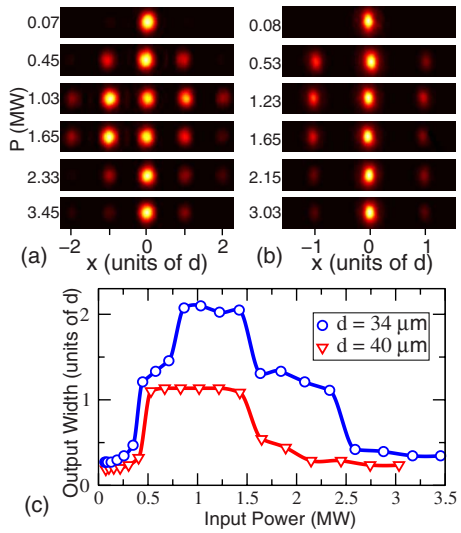

FIG. 4. (Color online) (a), (b) Output beam profiles as a function of input peak power, measured in curved laser-written waveguide arrays with waveguide spacing d=(a) 34 and (b) 40 μm. (c) Output beamwidth vs input power. Circles correspond to (a), triangles to (b).

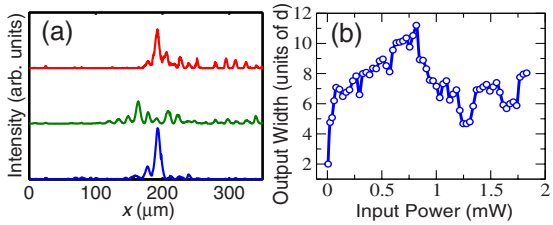

FIG. 5. (Color online) (a) Output intensity profiles measured in curved $LiNbO_3$ waveguide array for power levels of 6.1 μW, 0.85 mW, and 1.70 mW from bottom to top, respectively. (b) Output beamwidth vs input power (λ=532 nm).

see also Figs. 3(a) and 3(b)]. The error bars in Figs. 3(a) and 3(b) represent the uncertainty due to the laser power increments that we use in our measurements. However, there is also an additional uncertainty in the determination of the exact power for soliton formation due to the presence of weakly decaying oscillations of the beamwidth along the propagation direction. In Fig. 3(c) one can see that the self-induced beam broadening is less for the waveguide arrays with larger waveguide spacing, for which the coupling strength between the adjacent waveguides is lower. The maximum observed nonlinear beam broadening (diamonds) is less than the theoretical predictions (circles) calculated numerically. This is because the experiments are performed using short laser pulses while the numerical modeling is for the cw regime [15].

The results presented above are of generic nature and can possibly be observed in other physical systems, including charged particles in field-induced systems [13,21], and atomic BECs in optical lattices with repulsive interparticle interactions [7,20]. When only one site is excited at the input, the wave evolution should be in fact fully equivalent for both positive and negative nonlinearities, in the framework of the discrete tight-binding model [9,10,15,25]. In order to confirm that discrete diffraction-managed solitons can also form in curved waveguide arrays with defocusing nonlinearity [15], we have also performed experiments with curved $LiNbO_3$ waveguide arrays. The waveguides are fabricated by titanium indiffusion in a 50-mm-long X-cut $LiNbO_3$ crystal [25]. The light from a cw laser (λ=532 nm) is focused to a single waveguide of the array and the output intensity distribution is recorded on a charge-coupled device camera. The curved $LiNbO_3$ waveguide array, with a waveguide spacing d=14 μm, consists of two sections each L=25 mm long with bending amplitude A=24.5 μm. The bending amplitude has opposite signs in two successive array segments in order to improve the symmetry of the output beam profiles, as suggested originally in Ref. [12]. Similar to the case of focusing nonlinearity in silica glass, here we also observe that the self-collimation regime is destroyed and self-induced beam broadening takes place when the input power is increased. At higher powers, however, nonlinear beam self-trapping occurs. In Fig. 5 we show an example of this type of nonlinear dynamics. At low laser power (6.1 μW, linear regime) the output beam is confined to a single waveguide, positioned at a coordinate of 200 μm [Fig. 5(a), bottom profile]. Once the power is increased, the beam becomes strongly delocalized (middle intensity profile, 0.85 mW). However, for powers

above 1 mW most of the light is confined again to the input waveguide. The strong radiation on the right-hand side of the beam is a result of bending losses and coupling to higher-order bands through the effect of Zener tunneling. The dependence of the output beamwidth as a function of the input power is shown in Fig. 5(b) and matches qualitatively the power dependence predicted and observed for the self-focusing case.

In conclusion, we have observed experimentally the formation of discrete diffraction-managed spatial solitons in periodically curved waveguide arrays for both focusing and defocusing nonlinearities. The soliton formation occurs after transitional self-induced beam broadening, being fundamentally different from nonlinear self-focusing in bulk media or discrete self-trapping in straight waveguides. The critical power for the formation of lattice solitons in curved waveguide arrays is several times higher than the soliton power in straight waveguides, despite the reduction of the linear diffraction. These results open possibilities for independent control of the strength of diffraction and the nonlinear localization power, being applicable to different physical systems with attractive and repulsive nonlinear interactions.

[1] D. N. Christodoulides *et al.*, Nature (London) **424**, 817 (2003).
[2] D. N. Christodoulides and R. I. Joseph, Opt. Lett. **13**, 794 (1988).
[3] H. S. Eisenberg, Y. Silberberg, R. Morandotti, A. R. Boyd, and J. S. Aitchison, Phys. Rev. Lett. **81**, 3383 (1998).
[4] G. Lenz, I. Talanina, and C. M. de Sterke, Phys. Rev. Lett. **83**, 963 (1999).
[5] R. Morandotti, U. Peschel, J. S. Aitchison, H. S. Eisenberg, and Y. Silberberg, Phys. Rev. Lett. **83**, 4756 (1999).
[6] T. Pertsch, P. Dannberg, W. Elflein, A. Brauer, and F. Lederer, Phys. Rev. Lett. **83**, 4752 (1999).
[7] M. Gustavsson *et al.*, Phys. Rev. Lett. **100**, 080404 (2008).
[8] H. S. Eisenberg, Y. Silberberg, R. Morandotti, and J. S. Aitchison, Phys. Rev. Lett. **85**, 1863 (2000).
[9] S. Longhi, Opt. Lett. **30**, 2137 (2005).
[10] S. Longhi *et al.*, Phys. Rev. Lett. **96**, 243901 (2006).
[11] R. Iyer *et al.*, Opt. Express **15**, 3212 (2007).
[12] I. L. Garanovich, A. A. Sukhorukov, and Yu. S. Kivshar, Phys. Rev. E **74**, 066609 (2006).
[13] D. H. Dunlap and V. M. Kenkre, Phys. Rev. B **34**, 3625 (1986).
[14] M. J. Ablowitz and Z. H. Musslimani, Phys. Rev. Lett. **87**, 254102 (2001).
[15] I. L. Garanovich *et al.*, Opt. Express **15**, 9547 (2007).
[16] T. Pertsch *et al.*, Chaos **13**, 744 (2003).
[17] K. Staliunas, R. Herrero, and G. J. de Valcarcel, Phys. Rev. A **75**, 011604 (2007).
[18] I. R. Gabitov and S. K. Turitsyn, Opt. Lett. **21**, 327 (1996).
[19] M. Stratmann, T. Pagel, and F. Mitschke, Phys. Rev. Lett. **95**, 143902 (2005).
[20] B. A. Malomed, *Soliton Management in Periodic Systems* (Springer, New York, 2006).
[21] P. K. Datta and A. M. Jayannavar, Phys. Rev. B **58**, 8170 (1998).
[22] A. Szameit *et al.*, Opt. Express **13**, 10552 (2005).
[23] A. Szameit *et al.*, Opt. Express **15**, 1579 (2007).
[24] D. Blomer *et al.*, Opt. Express **14**, 2151 (2006).
[25] M. Matuszewski *et al.*, Opt. Express **14**, 254 (2006).